

Entropic sampling dynamics of the globally coupled kinetic Ising model

This article has been downloaded from IOPscience. Please scroll down to see the full text article.

2005 J. Phys. A: Math. Gen. 38 2115

(<http://iopscience.iop.org/0305-4470/38/10/004>)

View [the table of contents for this issue](#), or go to the [journal homepage](#) for more

Download details:

IP Address: 171.66.16.66

The article was downloaded on 02/06/2010 at 20:03

Please note that [terms and conditions apply](#).

Entropic sampling dynamics of the globally coupled kinetic Ising model

Beom Jun Kim¹ and M Y Choi^{2,3}

¹ Department of Molecular Science and Technology, Ajou University, Suwon 442-749, Korea

² Korea Institute for Advanced Study, Seoul 130-722, Korea

³ Department of Physics, Seoul National University, Seoul 151-747, Korea

E-mail: beomjun@ajou.ac.kr

Received 18 October 2004, in final form 26 January 2005

Published 23 February 2005

Online at stacks.iop.org/JPhysA/38/2115

Abstract

The entropic sampling dynamics based on the reversible information transfer to and from the environment is applied to the globally coupled Ising model in the presence of an oscillating magnetic field. When the driving frequency is low enough, coherence between the magnetization and the external magnetic field is observed; such behaviour tends to weaken with the system size. The time-scale matching between the intrinsic time scale, defined in the absence of the external magnetic field, and the extrinsic time scale, given by the inverse of the driving frequency, are used to explain the observed coherence behaviour.

PACS numbers: 05.40.–a, 75.10.Hk

1. Introduction

The stochastic resonance [1], which has been extensively studied in various systems including many-body systems⁴ [2–11], refers to the phenomenon that an appropriate amount of stochastic noise may not hinder but trigger the coherence between the output signal and the weak periodic input signal. In [11], a detailed study of the two-dimensional kinetic Ising model has been made and the size-dependence of the dynamic phase diagram has been identified. The globally coupled kinetic Ising model in the presence of a time-periodic external magnetic field has been investigated in detail, mainly because the simple mean-field method can be applied [4, 10]. In particular, the model has been recently shown to possess double stochastic resonance peaks at two distinct temperatures [6]. However, except for some systems [7], general applicability of the Glauber dynamics is hardly justified in many real systems.

The importance of the role of the entropy has been pointed out in the biological evolution [12]: in general, every species attempts to minimize its entropy, or in other words, to get

⁴ There have been attempts to justify the macroscopic Glauber dynamics of the classical Ising model from the microscopic quantum Hamiltonian. See, e.g., Martin P A 1977 *J. Stat. Phys.* **16** 149.

negative entropy from the environment. From this idea, it has been shown that the biological evolution of an ecosystem can be well described by the so-called entropic sampling dynamics [13]. We believe that the Ising model studied in this work can be related to a wide range of phenomena in biological and social systems, such as the opinion formation problem in social systems under the time-periodic influence [9]. Very recently, it has been suggested that the ubiquitously observed self-organized critical behaviour in nature is caused by the reversible information transfer with the surroundings of the system [14]. This implies that the entropic sampling dynamics, which is based on the reversible information exchange with the environment, can have realizations in many systems.

2. Entropic sampling dynamics of globally coupled Ising model

We in this work use the globally coupled Ising model, the Hamiltonian of which is given by

$$\mathcal{H} = -\frac{J}{2N} \sum_{i \neq j} \sigma_i \sigma_j - h \sum_i \sigma_i, \quad (1)$$

where $\sigma_i = \pm 1$ is the Ising spin at site i , J is the coupling strength, N is the total number of spins, and the external magnetic field h is coupled with the total magnetization $M \equiv \sum_i \sigma_i$. We first compute the entropy S by using the entropic sampling algorithm⁵ [13, 15], applied to the Hamiltonian in equation (1) at the constant magnetic field h . The detailed balance condition for the entropic sampling reads [13]

$$\frac{W(\vec{\sigma} \rightarrow \vec{\sigma}')}{W(\vec{\sigma}' \rightarrow \vec{\sigma})} = e^{-\{S[E(\vec{\sigma}')] - S[E(\vec{\sigma})]\}}, \quad (2)$$

where $W(\vec{\sigma} \rightarrow \vec{\sigma}')$ is the transition probability from $\vec{\sigma} \equiv \{\sigma_1, \sigma_2, \dots, \sigma_N\}$ to $\vec{\sigma}' \equiv \{\sigma'_1, \sigma'_2, \dots, \sigma'_N\}$, and for convenience, only a single spin is allowed to change at a given time. In the entropic sampling algorithm, one initially starts from $S(E) = 0$ for all values of the energy E , and obtains the histogram $H(E)$ for several Monte Carlo sweeps, which is then used to estimate a new value of $S(E)$:

$$S(E) = \begin{cases} S(E) & \text{for } H(E) = 0, \\ S(E) + \ln H(E) & \text{otherwise.} \end{cases} \quad (3)$$

As the above procedure continues, $S(E)$ approaches the true entropy up to an additive constant, which is independent of the energy E and thus may be subtracted on the condition that the minimum of $S(E)$ is zero.

Once the correct entropy is obtained, the time evolution under the entropic sampling should satisfy the detailed balance condition in equation (2) and we choose the following procedure: (1) Generate $\vec{\sigma}'$ which differs from $\vec{\sigma}$ only at one spin, e.g., $\vec{\sigma}' = \{\sigma_1, \sigma_2, \dots, -\sigma_j, \dots, \sigma_N\}$ obtained from $\vec{\sigma} = \{\sigma_1, \sigma_2, \dots, \sigma_j, \dots, \sigma_N\}$. (2) Compute the entropy change $\Delta S \equiv S[E(\vec{\sigma}')] - S[E(\vec{\sigma})]$. (3) If $\Delta S \leq 0$, accept the try, i.e., change $\vec{\sigma}$ to $\vec{\sigma}'$; otherwise, accept the try with the probability $e^{-\Delta S}$. One sweep of the above procedure for all the spins in the system corresponds to one time unit in the present work.

Figure 1 shows the entropy $S(E; h)$, computed for the system of size $N = 1600$ under time-independent field h , as a function of the energy per spin, $e \equiv E/N$ (henceforth, we measure the energy in units of the coupling strength J) obtained from 10^8 sweeps per spin. In the ground state all spins have the same value: $\sigma_i = 1$ if $h > 0$, and $\sigma_i = -1$ otherwise. Accordingly, the ground state energy is given by $E_{\text{ground}} = -N/2 - hN$ or $e_{\text{ground}} \equiv E_{\text{ground}}/N = -1/2 - h$. It is observed in figure 1 that $S(E; h) = 0$ for $e < e_{\text{ground}}$.

⁵ The entropy $S(E)$ can also be obtained efficiently from the Wang–Landau method of the flat histogram in [15].

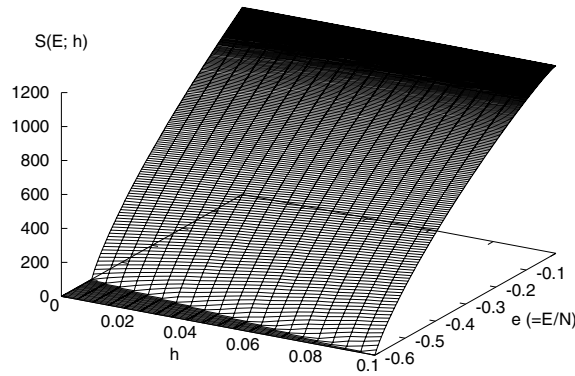


Figure 1. Entropy $S(E; h)$ as a function of the energy $e \equiv E/N$ per spin and the external magnetic field h . Each curve at a given value of h was obtained from the entropic sampling algorithm applied to the Hamiltonian in equation (1).

One can also compute $S(E; h)$ analytically as follows: from Stirling's series expansion, it is straightforward to get the entropy $S(m \equiv M/N)$ as a function of the magnetization,

$$S(m) \approx -N \left[\frac{1-m}{2} \ln \frac{1-m}{2} + \frac{1+m}{2} \ln \frac{1+m}{2} \right].$$

The entropy $S(E; h)$ is then obtained from equation (1) with $E/N = -m^2/2 - hm$. Since E is a quadratic function of m , $S(E; h)$ obtained in this way has two branches. In numerical simulations, we always observe only the upper branch, since it has a tremendously higher number of states than the lower branch. We confirmed that the numerically obtained $S(E; h)$ is in a good agreement with the upper branch of the analytic one. However, since Stirling's formula fails at $m = \pm 1$, we instead use the numerically obtained $S(E; h)$ for the time evolution of the system.

The entropy S is not a dynamic but a thermodynamic quantity. In the present work, we consider the case that the external magnetic field $h(t) = h_0 \sin(\Omega t)$ varies very slowly with time. In this low-frequency limit (i.e., the driving frequency Ω is sufficiently low), we may use the adiabatic approximation: at a given instant of time t , the entropy $S(E; h)$ computed above at the constant external field h is used for the time evolution of the system under the time-dependent field $h(t)$. In practice, $S(E; h)$ is computed at 100 different values of h in the range $0 \leq h \leq h_0$ with h_0 set equal to 0.1 throughout the work, and for a given value of $h(t)$, we choose $S(E; h)$ with the value of h closest to that of $h(t)$. From the symmetry of the Hamiltonian in equation (1), one has $S(E; -h) = S(E; h)$, which is utilized for the time evolution during the period $h(t) < 0$.

3. Results

The time evolution of the magnetization $m(t) \equiv M(t)/N = (1/N) \sum_i \sigma_i(t)$ is displayed in figure 2 for the system of size $N = 1600$ at driving frequencies $\Omega = (a) 0.005$, $(b) 0.02$, and $(c) 0.05$. Observed is the coherence behaviour at lower frequencies between $m(t)$ and $h(t)$, which may be explained in the following way: when $h(t) > 0$, the energy of the system is low for a larger value of $m(t)$. Since the entropy is a monotonically increasing function of the energy and since the entropic sampling dynamics tends to decrease the entropy, the positive value of $h(t)$ drives the system to have a larger value of $m(t)$, resulting in the coherence

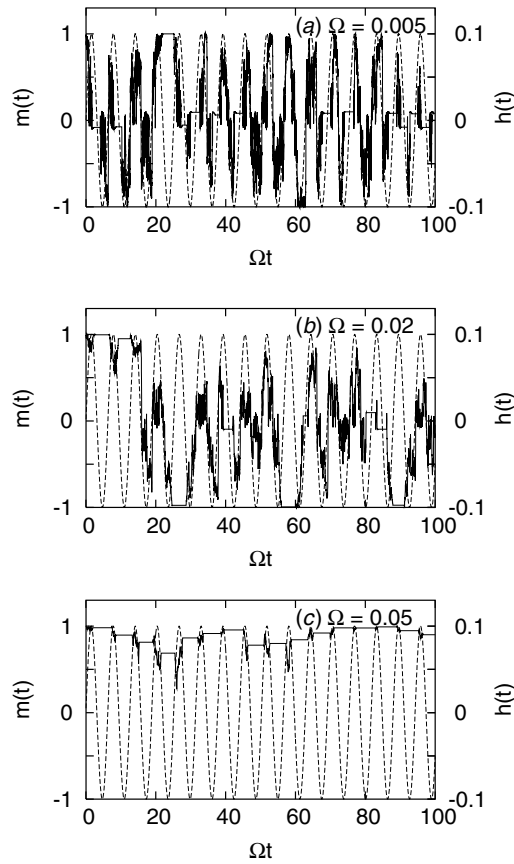


Figure 2. Entropic sampling time evolution of the magnetization $m(t)$ in a system of size $N = 1600$ at the driving frequency $\Omega = (a)$ 0.005, (b) 0.02 and (c) 0.05. Time series data have been obtained from the initial condition that all spins are aligned to have $m(t = 0) = 1$. For comparison, the time evolution of the external magnetic field $h(t) = h_0 \sin(\Omega t)$ with $h_0 = 0.1$ is also displayed (see the dashed lines). At sufficiently small values of Ω , $m(t)$ is observed to follow the external field $h(t)$ well. As Ω is raised, such coherence behaviour is shown to become weaker.

behaviour observed in figure 2. At small driving frequencies, the system has enough time to adjust itself to follow the external driving, and thus exhibits the coherence behaviour between the magnetization and the external driving well. On the other hand, as the driving frequency becomes higher, i.e., as the external driving changes in time too fast, the spins in the system do not have enough time to follow the driving $h(t)$.

Such coherence behaviour in figure 2, which we call *entropic coherence* to emphasize the role of the entropy, can be quantitatively detected by the occupancy ratio R , defined to be the average fraction of the spins in the direction of $h(t)$ [6, 16]:

$$R \equiv \left\langle \frac{\text{number of spins in the direction of } h(t)}{\text{total number of spins}} \right\rangle_t \quad (4)$$

with $\langle \dots \rangle_t$ denotes the time average. For the time sequence such as the one in figure 2(c), the occupancy ratio R has a value close to 1/2 since very few spins follow the driving $h(t)$ during the time period $h(t) < 0$. The occupancy ratio as a function of the driving frequency is displayed in figure 3 for the system of size $N = 1600$. As expected from figure 2, the

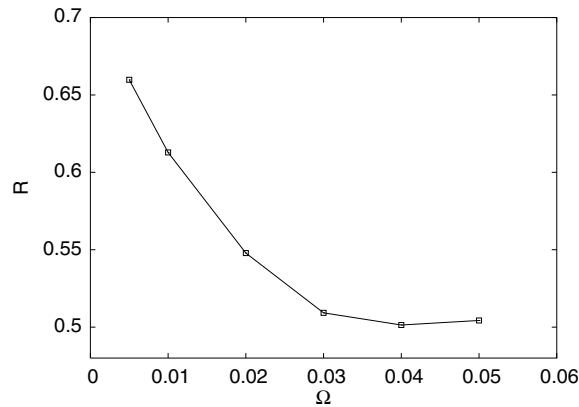


Figure 3. Occupancy ratio R as a function of the driving frequency Ω for the globally coupled Ising model of size $N = 1600$. As Ω becomes higher, coherence is observed to diminish: $R(\Omega) \rightarrow 0.5$ as Ω is increased.

occupancy ratio is observed to decrease with Ω and approaches the value $1/2$, signalling the disappearance of the coherence behaviour at higher frequencies.

From the above observation, it is expected that the competition of time scales should play an important role in the coherence behaviour. We use reasoning similar to that in the standard stochastic resonance [6] and identify the two time scales as follows: one is extrinsic and originates from the external driving frequency, and the other is intrinsic, in principle not depending upon the external driving. The extrinsic time scale $\tau_{\text{ext}} \equiv \Omega^{-1}$ reduces as the driving frequency Ω is increased, while the intrinsic time scale τ is fixed and independent of Ω . When $\tau_{\text{ext}} \gg \tau$, the system has enough time to relax and to follow $h(t)$, while in the opposite limit $\tau_{\text{ext}} \ll \tau$, spins cannot follow $h(t)$ which varies too fast. The intrinsic time scale τ , computed from the correlation function $\langle m(t)m(0) \rangle$ in equilibrium with the ensemble average $\langle \dots \rangle$, has been shown to follow the simple power law $\tau \sim N$ [14]. Qualitatively, one can also interpret τ as the time scale required to overcome the entropic barrier [17], separating $m = 1$ and $m = -1$.

Figure 4 shows the time evolution of the magnetization $m(t)$ in the presence of the external periodic driving $h(t) = h_0 \sin(\Omega t)$ with $\Omega = 0.01$ for the system size $N = (a) 400$, $(b) 1600$ and $(c) 2400$. As the size N is increased, the internal time scale τ grows, and eventually when τ becomes too large compared with τ_{ext} , the spins in the system cannot follow the external field. The behaviour of the occupancy ratio R with the size N is shown in figure 5 at external frequencies $\Omega = 0.01$ and 0.02 , which manifests the disappearance of the coherence behaviour as the system becomes larger⁶. Such behaviour may have interesting implications in sociological systems: social collective behaviour in accord with external driving may disappear quickly as the group size exceeds the critical value. In other words, the control by means of an external agent (e.g., laws or other social regulations) may become completely inefficient if the society grows too large. When this happens, enhancing interactions among people rather than strengthening social enforcement can be more effective for collective behaviour to emerge.

⁶ The origin of the non-monotonic behaviour at small sizes in figure 5 is not clear at this stage; it can be either due to a numerical artifact in the computation of the entropy $S(E; h)$, or it may originate from a generalized time-scale matching, i.e., the internal time scale, increasing with the system size N , matches with an integer multiple of the external time scale.

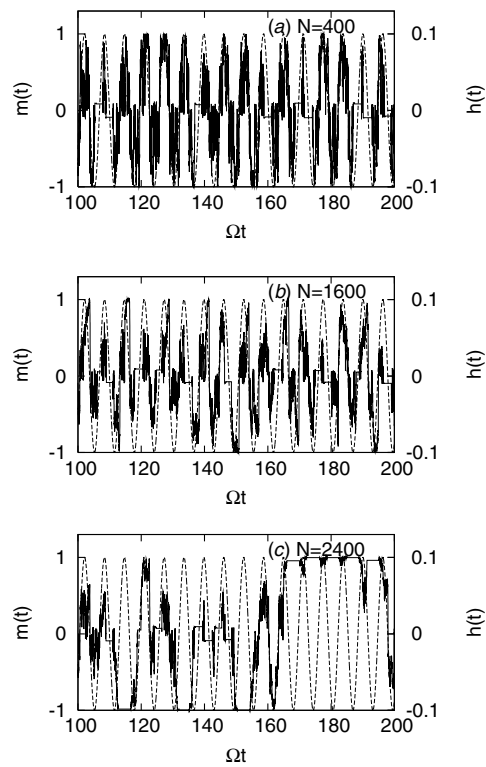


Figure 4. Entropic sampling time evolution for the globally coupled Ising model at the driving frequency $\Omega = 0.01$ for size $N = (a) 400$, $(b) 1600$ and $(c) 2400$. As N is increased, the coherence behaviour becomes weaker.

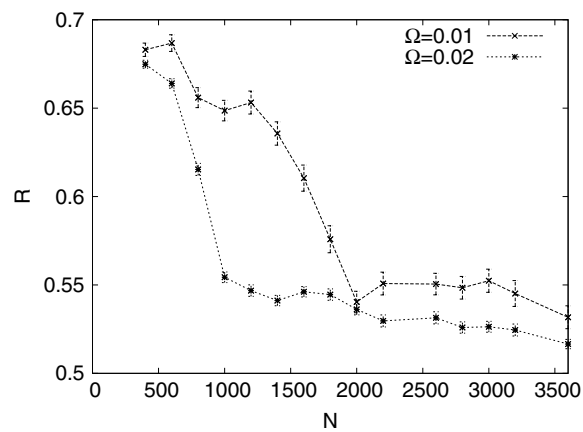


Figure 5. Occupancy ratio R versus the system size N at the driving frequency $\Omega = 0.01$ and 0.02 . As N is increased, the entropic coherence becomes weaker and gradually disappears in sufficiently large systems.

4. Conclusion

In summary, we have studied the coherence behaviour in the globally coupled Ising system under a time-periodic external magnetic field. The entropic sampling algorithm has been used both for the calculation of the entropy and for the time evolution of the system. When the external driving frequency is sufficiently low (namely, when the external field varies slowly with time) and when the system is not too large, the coherence behaviour between the magnetization and the external field has been observed. It seems appropriate to call this phenomenon entropic coherence, which emphasizes the role of the entropy in the time evolution. It is noteworthy that if one uses a similar entropic sampling time evolution for the entropy as a function of, e.g., the magnetization $S(M)$ instead of the energy, we do not have the coherence behaviour: $S(M)$ can be computed from a purely combinatorial counting problem and accordingly, does not reflect the presence of the external magnetic field in the Hamiltonian (1). It is plausible that this entropic coherence idea may be used to explain the coherence behaviour of those systems the dynamics of which are more appropriately described by the entropy. The importance of the entropy has been pointed out in the description of the biological evolution [12] and the resulting dynamics has been suggested to be of wide applicability to a variety of the self-organized critical systems [14]. Accordingly, we believe that the present work can be extended to explain, e.g., various social and biological systems in the presence of periodic external driving coupled with the internal degrees of freedom.

Acknowledgments

This work was supported in part by KOSEF Grant No. R14-2002-062-01000-0, by the Hwang-Pil-Sang research fund (BJK), and by the BK21 Program (MYC). Numerical simulations were performed on the computer cluster Iceberg at Ajou University.

References

- [1] Gammaitoni L, Hänggi P, Jung J and Marchesoni F 1998 *Rev. Mod. Phys.* **70** 223
- [2] Lindner J F, Meadows B K, Ditto W L, Inchiosa M E and Bulsara A R 1995 *Phys. Rev. Lett.* **75** 3
Marchesoni F, Gammaitoni L and Bulsara A R 1996 *Phys. Rev. Lett.* **76** 2609
Kim S, Park S H and Pyo H-B 1999 *Phys. Rev. Lett.* **82** 1620
Hong H and Choi M Y 2000 *Phys. Rev. E* **62** 6462
- [3] Néda Z 1995 *Phys. Rev. E* **51** 5315
Néda Z 1996 *Phys. Lett. A* **210** 125
Leung K-T and Néda Z 1999 *Phys. Rev. E* **59** 2730
- [4] Leung K-T and Néda Z 1998 *Phys. Lett. A* **246** 505
- [5] Kim B J, Choi M-S, Minnhagen P, Jeon G S, Kim H J and Choi M Y 2001 *Phys. Rev. B* **63** 104506
Jeon G S, Kim H J, Choi M Y, Kim B J and Minnhagen P 2002 *Phys. Rev.* **65** 184510
Jeon G S, Lim J S, Kim H J and Choi M Y 2002 *Phys. Rev.* **66** 024511
- [6] Kim B J, Minnhagen P, Kim H J, Choi M Y and Jeon G S 2001 *Europhys. Lett.* **56** 333
- [7] Park K, Novotny M A and Rikvold P A 2002 *Phys. Rev. E* **66** 056101
- [8] Hong H, Kim B J and Choi M Y 2002 *Phys. Rev. E* **66** 011107
- [9] Kuperman M and Zanette D 2002 *Euro. Phys. J. B* **26** 387
- [10] Tomé T and de Oliveira M J 1990 *Phys. Rev. A* **41** 4251
Lo W S and Pelcovits R A 1990 *Phys. Rev.* **42** 7471
Acharyya M and Chakrabarti B K 1995 *Phys. Rev. B* **52** 6550
Sides S W, Rikvold P A and Novotny M A 1998 *Phys. Rev. Lett.* **81** 834
Sides S W, Rikvold P A and Novotny M A 1999 *Phys. Rev. E* **59** 2710
- [11] Korniss G, Rikvold P A and Novotny M A 2002 *Phys. Rev. E* **66** 056127
- [12] Choi M Y, Lee H Y, Kim D and Park S H 1997 *J. Phys. A: Math. Gen.* **30** L749

-
- [13] Lee J 1993 *Phys. Rev. Lett.* **71** 211
Lee J and Choi M Y 1994 *Phys. Rev. E* **50** R651
 - [14] Choi M Y, Kim B J, Yoon B-G and Park H 2005 *Europhys. Lett.* **69** 503
 - [15] Wang F and Landau D P 2001 *Phys. Rev. Lett.* **86** 2050
 - [16] Lindner J F, Meadows B K, Ditto W L, Inghiosa M E and Bulsara A R 1995 *Phys. Rev. Lett.* **75** 3
 - [17] Ritort F 1995 *Phys. Rev. Lett.* **75** 1190
Kim B J, Jeon G S and Choi M Y 1996 *Phys. Rev. Lett.* **76** 4648